JLB

Article

Receptor cleavage and P-selectin-dependent reduction of leukocyte adhesion in the spontaneously hypertensive rat

Angela Y. Chen,[1] Jessica N. Ha, Frank A. DeLano, and Geert W. Schmid-Schönbein

Department of Bioengineering, Institute of Engineering in Medicine, University of California, San Diego, La Jolla, California, USA

RECEIVED JANUARY 10, 2012; REVISED MARCH 22, 2012; ACCEPTED APRIL 13, 2012. DOI: 10.1189/jlb.0112010

ABSTRACT

The SHR, a genetic model for hypertension and the metabolic syndrome, has attenuated leukocyte adhesion to the postcapillary endothelium by an unknown mechanism. Based on recent evidence of elevated levels of MMPs in plasma and on microvascular endothelium of the SHR with cleavage of several receptor types, we hypothesize that the reduced leukocyte-endothelial interaction is a result of enhanced proteolytic cleavage of P-selectin on the postcapillary endothelium and PSGL-1 on leukocytes. The attenuated rolling interactions of SHR leukocytes with the endothelium were restored by chronic treatment with a broad-spectrum MMP inhibitor (CGS) for 24 weeks. The SHR MMP levels, in plasma and mesentery, as well as the systolic blood pressure, decreased significantly with treatment. In the SHR mesentery, labeling of P-selectin in the postcapillary venules by immunohistochemistry demonstrated, on average, a 31% lower extracellular P-selectin density compared with the normotensive WKY. A significantly lower extracellular PSGL-1 density on the membranes of SHR neutrophils compared with the WKY also supported our hypothesis. In vivo stimulation of the mesenteric postcapillary venules with histamine demonstrated that the SHR had an attenuated response, as measured by leukocyte rolling velocity on the endothelium. The reduced P-selectin and PSGL-1 density, on SHR postcapillary endothelium and on SHR leukocytes, respectively, was restored significantly by chronic MMP inhibition. The impaired ability of SHR leukocytes to reduce rolling velocity upon inflammatory stimulation led to fewer firmly adhered leukocytes to the endothelium as a contributor to immune suppression. *J. Leukoc. Biol.* 92: 183–194; 2012.

Introduction

Recruitment of leukocytes to the endothelium in postcapillary venules during inflammation is a multistep process. It begins with displacement of leukocytes onto the endothelium by hydrodynamic interaction with erythrocytes and membrane rolling of leukocytes on the endothelium, followed by firm adhesion, spreading, crawling, and eventual leukocyte migration across the endothelium into tissue [1]. The leukocyte adhesion cascade involves selectins, integrins, chemokines, and kinases [1] and is also under the control of fluid shear stress. When stimulated, P-selectin serves as a transient adhesion receptor on the surface of endothelial cells. Its primary counter-receptor, PSGL-1, on the surface of leukocytes, binds to P-selectin and facilitates rolling along the endothelium with subsequent adhesion and extravasation [2, 3]. Mice deficient in selectins have increased circulating leukocyte counts as a result of the leukocytes' inability to roll on the endothelium, resulting in reduced migration of T lymphocytes into inflamed tissue [4].

Besides elevated blood pressure and insulin resistance, the SHR exhibits multiple signs of immune suppression with a reduced inflammatory response [5]. The SHR has a chronic elevation of circulating leukocyte count [6] with enhanced formation of pseudopods and lengthened transit time through capillaries, thereby resulting in elevated capillary hemodynamic resistance [7]. In addition, the SHR has a defective adhesion of leukocytes to postcapillary endothelium [8] and exhibits enhanced apoptosis of lymphocytes in the thymus [9]. With elevated MMP levels, specifically MMP-2, -7, and -9, in the plasma and on arteriolar and venular endothelium of the microcirculation [10, 11], the SHR has been found to have excessive cleavage of several membrane receptors, such as the insulin receptor-α, VEGFR-2, FPR, β_2-adrenergic receptor, as well as β_2-integrin leukocyte adhesion receptor (CD18) [10–13]. Abnormal cleavage of these receptors has been shown to result in insulin resistance, capillary rarefaction, reduced neutrophil fluid shear stress response (hemodynamic resistance),

Abbreviations: $^{-/-}$=knockout, CGS=CGS27023A, a broad-spectrum matrix metalloproteinase inhibitor, CGS SHR=CGS27023A-treated spontaneously hypertensive rat, CGS WKY=CGS27023A-treated Wistar Kyoto rat, dH_2O=distilled water, MMP=matrix metalloproteinase, PSGL-1=P-selectin glycoprotein ligand-1, s=soluble, SHR=spontaneously hypertensive rat, t=time, vWF=von Willebrand factor, WKY=Wistar Kyoto rat

1. Correspondence: Department of Bioengineering, Institute of Engineering in Medicine, University of California, San Diego, 9500 Gilman Dr., La Jolla, CA 92093-0412, USA. E-mail: ayc015@ucsd.edu

0741-5400/12/0092-183 © Society for Leukocyte Biology

arteriolar constriction, and systemic hypertension, respectively [10–13]. As proteolytic cleavage may affect other membrane receptors, we examine in this study how elevated MMP levels may interfere with mechanisms of P-selectin-mediated leukocyte adhesion in the SHR.

Upon histamine stimulation, selectin-mediated leukocyte adhesion to the venular endothelium is impaired in the SHR [8]. The phenomenon is associated with a reduced venular expression of P-selectin in the SHR [8], leading to an elevated number of circulating leukocytes, including PMN leukocytes [14]. Compared with normotensive rats, leukocytes in the mesenteric postcapillary venules of hypertensive rats also show reduced adhesion and emigration upon stimulation with platelet-activating factor or leukotriene B_4 [14]. We hypothesize that the attenuated leukocyte adhesion and rolling on mesenteric postcapillary endothelium are a result of proteolytic cleavage of P-selectin and PSGL-1 by elevated levels of MMPs.

We tested the hypothesis by measurements of the extracellular P-selectin density on endothelial cells of mesenteric microvessels of the WKY and SHR via whole-mount mesentery immunohistochemistry and in the form of sP-selectin in plasma by ELISAs. We also quantified the density of PSGL-1 on neutrophils by immunolabeling intracellular and extracellular domains. As a functional test, we performed in vivo intravital experiments, where SHR leukocyte rolling velocities were tracked along the mesenteric endothelium upon histamine stimulation. MMP activity in WKYs and SHRs was blocked with a broad-spectrum MMP inhibitor (CGS; 3 mg/kg/day) [15] in their drinking water for 24 weeks as a pharmacological intervention.

MATERIALS AND METHODS

Animals

All animal protocols were reviewed and approved by the Institutional Animal Care and Use Committee at the University of California, San Diego (CA, USA). Control SHR and WKY rats (8 weeks of age; male; Harlan Laboratories, Indianapolis, IN, USA; n=5) were given standard diet and drinking water ad libitum, whereas a separate, age-matched treatment group (male; denoted CGS SHR and CGS WKY; n=7) was given 3 mg/kg/day of the broad-spectrum MMP inhibitor CGS {also known as MMI270; N-hydroxy-2(R)-[(4-methoxysulfonyl) (3-picolyl)-amino]-3-methylbutaneamide hydrochloride monohydrate; Novartis Pharmaceuticals, Summit, NJ, USA} in its drinking water. The 3-mg/kg/day CGS dose was based on the effective antimetastatic dose (5–25 mg/kg) for a mouse melanoma model via osmotic pump; however, our treatment was administered in the drinking water, and we found that a lower dose was necessary to enhance drug consumption and maintain normal drinking of the inhibitor-containing water [15]. The treatment duration of 24 weeks was the time required for the MMP activity in the SHR plasma to decrease significantly and the SHR blood pressure to lower (SHR vs. CGS SHR groups). Prior to 24 weeks, we checked the systolic blood pressure and plasma MMP activity at various time-points and found no significant differences between SHR and CGS SHR groups.

In vivo MMP assay and leukocyte rolling experiments

The rats were tranquilized with a s.c. injection of 10 mg/kg body weight of xylazine (Vedco, St. Joseph, MO, USA), followed after 15 min by an intramuscular injection of 50 mg/kg body weight of sodium pentobarbital (Abbott Laboratories, North Chicago, IL, USA) at the rats' caudal thigh muscle of the hind limb for general anesthesia. Supplemental doses of sodium pentobarbital at 5 mg/kg body weight were given i.v. as needed after cannulation of the femoral vein (polyethylene catheters, PE50; Becton Dickinson Primary Care Diagnostics, Sparks, MD, USA).

A midline abdominal incision was made. The mesentery was gently placed outside of the abdominal cavity using dampened cotton swabs and prepared on a glass pedestal, while superfused with Krebs-Henseleit solution and gassed with 5% carbon dioxide and 95% nitrogen. Images of the mesentery were recorded with a digital fluorescent intravital microscope (Leica, Buffalo Grove, IL, USA) using a 10× water immersion microscope objective (Leica; numerical aperture 0.3) and a 10× eyepiece. Cotton gauze was used to lightly pin down a mesentery sector.

For MMP activity detection, we topically applied the broad-spectrum MMP substrate solution {7-methoxycoumarin-4-acetyl-Pro-Leu-Gly-Leu-β-(2,4-dinitrophenylamino) Ala-Arg amide; Sigma-Aldrich, St. Louis, MO, USA; #M6412; 2 μmol/L [16]} to the mesentery, prepared as described above (of WKY, SHR, CGS WKY, and CGS SHR; n=5 for each group), following removal of Krebs-Henseleit solution via gentle suction. The 7-methoxycoumarin group of the substrate is quenched by energy transfer to the 2,4-dinitrophenyl group, and cleavage of the Gly-Leu bond produces a fluorescent signal (328/393 nm) [16]. This MMP fluorogenic substrate is cleaved by collagenases, stromelysins, and 72 kDa gelatinase [16]. Fluorescent images of the mesentery submerged in the substrate solution were captured at Time 0 (when the substrate was applied initially with minimal incubation) and at a 1-h incubation. Images of the mesentery without substrate and of the substrate alone served as negative controls. The intensity of the emitted fluorescent light was recorded in digital units (0–255, where 0 is pure black, and 255 is pure white) after subtraction of background intensity at Time 0, using consistent microscope and camera settings. Postcapillary venules and arterioles were distinguished by tracing upstream or downstream of capillaries in the mesentery and locating arteries surrounding individual mesentery sectors. Vessel-wall thickness and diameters also facilitated the distinction.

For leukocyte rolling measurements, video records of leukocytes in postcapillary venules were made after 20 min of equilibration until hemodynamic parameters reached steady-state. Bright field images (3 min in duration) of postcapillary venules on rat mesentery were captured and stored (on DVD) every 10 min over a time course of over 1 h, using a 60× water immersion objective (Leitz, now Leica). Leukocyte velocity was measured by tracking frame-by-frame cell positions along an 80-μm segment of a venule and dividing by the time each cell required to traverse the vessel segment. Leukocyte rolling velocities, V_W, were normalized by erythrocyte velocities, V_R, as follows

$$\mathrm{I_{mas}} = \frac{V_W}{V_R},$$

$\mathrm{I_{mas}}$ is an index of the strength of the membrane-adhesive energy between leukocytes and the endothelium [8].

We used a velocimeter (Velocity Tracker MOD-102; IPM, La Mesa, CA, USA) to measure centerline erythrocyte velocity, V_R, calibrated by a rotating glass disc [17]. The mean erythrocyte velocity (V_{mean}) was computed as

$$V_{mean} = \frac{V_R}{1.6},$$

,

where V_R represents centerline erythrocyte velocity in the venule [8]. The venular wall shear rate on the endothelium was computed as

$$\gamma = 8 * \left(\frac{V_{mean}}{D_v} \right),$$

where V_{mean} and D_v represent average erythrocyte velocity and venular diameter, respectively [8].

The shear rate was recorded in individual, unbranched vessels (25–40 μm in diameter) every 7 min, using a 3-min record ending at 60 min. A leukocyte was defined to be adherent to the endothelium when it was stationary and not rolling for at least 30 s. To observe leukocyte rolling in the

presence of histamine, we removed the Krebs-Henseleit superfusate on the mesentery and applied 10 μmol/L histamine dihydrochloride (Sigma-Aldrich; #53300 as a stimulant of P-selectin) in 1× PBS at t = 0 min for 10 min. Five animals (n=5), in each of the following groups, were studied: SHRs, WKY rats, CGS SHRs, and CGS WKY rats (20 cells/rat analyzed). At the end of the study, the animals were euthanized (120 mg/kg Fatal Plus, i.v.; Vortech Pharmaceuticals, Dearborn, MI, USA).

Superfusion of MMP-9 on WKY mesenteric postcapillary venules in vivo

As a positive control, to determine specific MMPs responsible for proteolytic cleavage of P-selectin, we topically applied 1.63 nM MMP-9 to WKY mesentery after 10 min of 10 μM histamine stimulation with the same mesenteric preparation described above (n=3 rats). Histamine not only induces P-selectin on endothelial cells, but it also acts as a vasodilator, which increases permeability of microvessels. The 1.63-nM MMP-9 concentration is based on plasma MMP-9 levels measured from hypertensives [18]. Video recordings of adherent leukocytes on an 80-μm segment of the WKY postcapillary venule were made on DVDs at the following time-points: (1) t = 0: immediately prior to histamine stimulation; (2) t = 10 min: at the end of 10 min histamine stimulation, immediately followed by MMP-9 superfusion; (3) t = 20 min: at the end of 10 min MMP-9 superfusion. Negative controls with 1× PBS in place of MMP-9 superfusion were included (n=3 WKY rats).

Blood collection and PSGL-1 labeling by immunohistochemistry

Blood (100 μl) was collected via a great saphenous vein puncture and heparinized (10 U/ml) to prevent coagulation. Blood smears were made with 10 μl blood (n=4) on glass slides (Fisher Scientific, Pittsburgh, PA, USA; #12-544-7) and fixed in 10% neutral-buffered formalin (Fisher Scientific; #23-032-060) in the following groups: SHRs, WKY rats, CGS SHRs, and CGS WKY rats. A hydrophobic pen (Vector Laboratories, Burlingame, CA, USA; #H-4000) was used to define borders for the labeling area.

The blood smears were incubated for 5 min in 0.5% hydrogen peroxide (to block endogenous peroxidase activity; Sigma-Aldrich; #H-1009; diluted in tap water) and 2.5% normal horse serum (to prevent nonspecific binding; Vector Laboratories; #MP-7405; ImPRESS reagent anti-goat Ig peroxidase kit), respectively. Primary antibodies targeting the extracellular domain (Santa Cruz Biotechnology, Santa Cruz, CA, USA; sc-10174; 12 μg/ml final concentration) or intracellular domain (Santa Cruz Biotechnology; sc-10176; 12 μg/ml final concentration) of PSGL-1 were applied for 90 min. For negative control, normal goat IgG (Santa Cruz Biotechnology; # sc-2028; 12 μg/ml final concentration) was applied in place of the primary antibody. Following primary antibody, secondary antibody conjugated to peroxidase (Vector Laboratories; #MP-7405; ImPRESS reagent anti-goat Ig peroxidase kit) was applied to the blood smears for 30 min. Lastly, Vector NovaRED, which is a substrate for peroxidase, was applied for 5 min (Vector Laboratories; #SK-4800), and a color change in red served as the reporter for antibody binding to PSGL-1. We used 1× PBS as the wash buffer to remove excess antibodies and reagents in between steps for the above procedure.

Blood pressure measurements

After 24 weeks of treatment with CGS, we measured the systolic blood pressure of the treated SHR and WKY rats via tail-cuff plethysmography. The tail-cuff is set up with a balloon-pressure controller and a Power Lab channel apparatus (AD Instruments, Colorado Springs, CO, USA). The systolic blood pressures of n = 7 rats/group of the treated animals (CGS WKY and CGS SHR) and n = 5 rats of the nontreated or control animals (WKY and SHR) were measured.

In vitro gelatinase assay

To determine the blood plasma gelatinase level after chronic CGS treatment of the SHR and WKY rat groups, we used the EnzChek Gelatinase/Collagenase Assay Kit (Life Technologies, Carlsbad, CA, USA; #E-12055). Gelatin (final concentration at 10 μg/ml), from pig skin conjugated to fluorescein, served as the substrate (digestion product generates signal with λ_{ex}=495 nm and λ_{em}=515 nm). Blood was collected from animals treated with CGS by great saphenous vein puncture and centrifuged at 400 g and 4°C for 10 min. We used 50 μl plasma for each sample in the assay, and an equal volume of 1× kit reaction buffer as the plasma diluent. We generated a standard curve using collagenase from *Clostridium histolyticum*, provided by the kit, as positive control. A spectrophotometer (FilterMax F5 Multi-Mode Microplate Reader; Molecular Devices, Sunnyvale, CA, USA) was used to read the fluorescence from the gelatinase reactions. Gelatinase activity in the plasma of SHRs, WKY rats, CGS WKY rats, and CGS SHRs (n=3 animals/group) was analyzed. The fluorescence of reaction samples was read initially after enzyme and substrate mixing and then every 5 min for a total of 20 min. The increase in enzyme activity over time was used for comparison among groups.

P-selectin labeling on whole-mount mesentery by immunohistochemistry

After completion of in vivo studies and euthanasia, we collected the mesentery sectors along with the cecum and intestines by cecal ligation, excision, and subsequent fixing of the mesentery in 10% neutral-buffered formalin (Fisher Scientific, Pittsburgh, PA; #23-032-060) overnight. Individual mesentery sectors were excised the next day and washed with tap water and 0.5% hydrogen peroxide (to block endogenous peroxidase activity) in 10 ml glass beakers. Digest-All 4 Proteinase K Solution (Life Technologies; #00-3011) was used to permeabilize the mesentery and allow for penetration and binding of antibodies. This step was followed by application of 2.5% normal horse serum (Vector Laboratories; #MP-7405; ImPRESS reagent anti-goat Ig peroxidase kit) to block nonspecific binding. After washing with 1× PBS (Sigma-Aldrich; #P5493, diluted in dH_2O), the mesentery sector was incubated with primary antibody targeting an epitope in the extracellular domain of P-selectin (R&D Systems, Minneapolis, MN, USA; #AF737; goat-anti-mouse CD62P antibody; homology of mouse vs. rat is 78%; final concentration in 1× PBS is 12 μg/ml) for 2 h. The secondary antibody (Vector Laboratories; #MP-7405; ImPRESS reagent anti-goat Ig peroxidase kit) was applied for another 2 h, and excess antibody was removed by rinsing in 1× PBS. The mesentery was then incubated in Vector NovaRED (Vector Laboratories; #SK-4800) for 1 min. The mesentery was washed in dH_2O, mounted on a glass slide to dry overnight, coverslipped with Vecta-Mount mounting media (Vector Laboratories; #H-5000), and allowed to dry another day before microscope imaging.

We used an inverted microscope (Olympus IX70) with a 40× objective to observe the whole-mount, labeled mesentery. Quantitative analysis of P-selectin label density was determined from the images under the 40× objective. Images were captured with a charge-coupled device camera (Optronics) using WinTV 2000 camera software (Version 3.55.21090, Hauppauge Computer Works, Hauppauge, NY, USA).

Circulating leukocyte count

Blood was drawn from femoral artery, and Unopette #365804 capillary pipette (20 μl) microcollection system for leukocyte count (dilution factor 100) was used (Becton Dickinson, Franklin Lakes, NJ, USA). Red blood cells in whole blood were lysed in 0.0268% acetic acid provided in the collection tube, and leukocytes were counted with a hemocytometer. Leukocyte differentials (including PMN leukocytes and lymphocytes) of WKY, SHR, CGS WKY, and CGS SHR (n=7) were recorded using 40× microscope objective.

Plasma sP-selectin ELISA

A rat sP-selectin ELISA kit was purchased from Novatein Biosciences (Cambridge, MA, USA; #NB-E30415). Plasma samples from WKY, SHR, CGS WKY, and CGS SHR (n=3) were analyzed based on kit protocol.

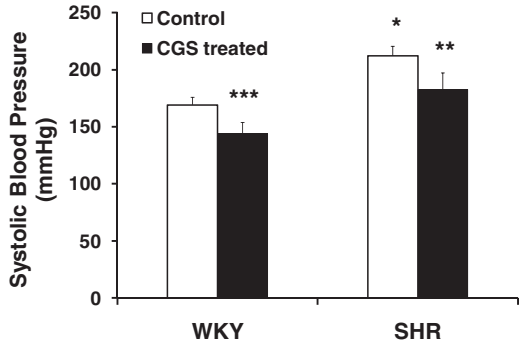


Figure 1. Systolic blood pressure of WKY, SHR, CGS WKY, and CGS SHR, as measured by tail-cuff plethysmography (n=5 for WKY and SHR; n=7 for CGS WKY and CGS SHR). Ten consecutive blood pressure measurements were made and averaged for each animal. One-tailed Student's t test: *$P < 0.01$ WKY versus SHR; **$P < 0.01$ SHR versus CGS SHR; ***$P < 0.01$ WKY versus CGS WKY. Single-factor ANOVA: $P < 0.01$ among WKY, SHR, CGS WKY, and CGS SHR (not shown).

Measurements and analysis of in vivo leukocyte rolling velocities

Leukocyte rolling velocities were measured from video records of mesenteric postcapillary venules via frame-by-frame measurements of the time interval that leukocytes require to traverse along an 80-μm venular segment before, during, and after histamine stimulation (a P-selectin stimulant).

Measurements of adherent leukocyte count

The number of leukocytes along 80 μm postcapillary venular segments stationary for 30 s was considered adherent to the endothelium and counted. For the positive control experiment, where MMP-9 was superfused on WKY mesenteric postcapillary venules, the normalized adherent leukocyte count was computed by dividing the number of adherent leukocytes at the end of MMP-9 superfusion (t=20 min) by that before MMP-9 superfusion (t=10 min).

Quantification of in vivo MMP activities

Images of the mesenteric microvessels were captured of the fluorescence emitted by the fluorogenic MMP substrate, which reported the presence of MMPs in vivo. Fluorescent intensities were traced digitally along a contour line on the endothelial cells of mesenteric microvessels. MMP activity was determined in the form of average pixel intensity using digital image analysis (ImageJ, Version 1.42q).

Quantification of PSGL-1 density on neutrophil membranes

Images showing immunohistochemical labeling of PSGL-1 on blood smears (derived from Vector NovaRED substrate) were analyzed by tracing contours of neutrophils and by measurements of the average pixel intensity on each cell within the contours. The OD (dimensionless) for the PSGL-1 label was then computed as described previously [13].

Quantification of P-selectin density on mesenteric microvessels

Images of whole-mount mesentery immunohistochemical labels for P-selectin were analyzed by first splitting the original micrograph into its red, blue, and green channels (ImageJ, Version 1.42q). As red channel images show the signals from Vector NovaRED substrates, they were used for measurements of P-selectin label intensity. A contour was drawn around each mesenteric microvessel. The mean pixel intensity was determined within each vessel contour (10 venular, 10 capillary, as well as 10 arteriolar segments were measured and averaged/animal; five animals were analyzed in each group: WKY, SHR, CGS WKY, and CGS SHR).

Statistical analysis

Experimental results are reported as mean ± SD. We used single-factor ANOVA (Microsoft Excel 2007) for comparisons among experimental groups >2. One-tailed Student's t test was used to evaluate the differences between any two experimental groups. $P < 0.05$ was considered statistically significant in Student's t test and single-factor ANOVA.

RESULTS

Chronic MMP inhibition with the broad-spectrum MMP inhibitor CGS led to the normalization of systolic blood pressure in the SHR

After 24 weeks of CGS treatment in their drinking water, the SHR's elevated systolic blood pressure (**Fig. 1**; WKY vs. SHR) was reduced significantly (Fig. 1; SHR vs. CGS SHR). The systolic blood pressure of CGS WKY was also reduced significantly from that of the WKY (Fig. 1; WKY vs. CGS WKY). Furthermore, the systolic blood pressure of the CGS SHR group was, on average, not significantly different from the WKY controls.

Chronic MMP inhibition with the broad-spectrum MMP inhibitor CGS reduced the MMP activity in the SHR

The elevated plasma gelatinase activity in the SHR compared with the WKY was reduced significantly by CGS treatment (**Fig. 2**; SHR vs. CGS SHR). In addition, CGS WKY plasma gelatinase levels

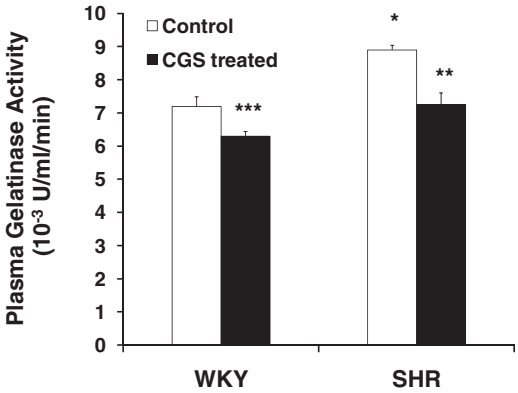


Figure 2. Plasma gelatinase activity for WKY, SHR, CGS WKY, and CGS SHR (n=3 rats/group), measured in a fluorescent spectrophotometer over time. The substrate is gelatin-conjugated to fluorescein, and gelatinase activity is proportional to fluorescence produced from enzymatic reactions. One-tailed Student's t test: *$P < 0.05$ WKY versus SHR; **$P < 0.05$ SHR versus CGS SHR; ***$P < 0.05$ WKY versus CGS WKY. Single-factor ANOVA: $P < 0.01$ among WKY, SHR, CGS WKY, and CGS SHR (not shown). One unit (U) is defined as the amount of enzyme required to liberate 1 μmole/L L-leucine equivalents from collagen in 5 h at 37°C and pH 7.5 based on Life Technologies manual (#E-12055).

were significantly lower than that of the WKY. Plasma gelatinase activity of the CGS SHR group was not significantly different from the WKY controls (Fig. 2). The in vivo MMP activity, as detected with a broad-spectrum MMP fluorogenic substrate along mesenteric postcapillary venules, as well as arterioles, is significantly higher in the SHR than the WKY (**Fig. 3A–C**). On average, the MMP activity is 37% higher in the postcapillary venules (Fig. 3B) and 24% higher in the arterioles (Fig. 3C) of the SHR compared with the WKY. After chronic inhibition, the MMP activity in the CGS SHR group was significantly lower compared with the SHR group (Fig. 3A–C). In a similar manner, the average MMP activity in CGS WKY was reduced significantly from that in the WKY (Fig. 3A–C).

With blunted responses to histamine stimulation, the SHR presented impaired leukocyte rolling and adhesion mechanisms, which were restored by chronic MMP inhibition

With histamine stimulation (10 μmol/L) inducing P-selectin expression at Time 0 (for 10 min), the leukocyte rolling velocity (relative to centerline erythrocyte velocity) of the normotensive WKY rat responded with a reduction of leukocyte rolling velocity, followed by a recovery period (**Fig. 4A**). In contrast, the SHR revealed an attenuated reduction of leukocyte rolling velocity following histamine stimulation (Fig. 4A). The normalized leukocyte rolling velocity for the SHR is significantly higher than that in the WKY at Time 30 min (Fig. 4A). With chronic MMP inhibition by CGS, the SHR response to histamine is restored (Fig. 4A). In the postcapillary venules, the WKY transiently increased the venular shear rate after histamine stimulation, whereas the SHR did not (Fig. 4B). In the interval from 10 min to 50 min (t=10–50 min), after the onset of histamine stimulation (t=0 min), the number of adherent leukocytes was significantly lower in the SHR compared with the WKY (Fig. 4C). Chronic MMP inhibition restored the number of adherent leukocytes in the SHR (Fig. 4C, CGS SHR vs. SHR). At t = 10, 20, 30, and 40 min, the average number of adherent leukocytes on the postcapillary venular endothelium is significantly higher in the CGS SHR than the SHR (Fig. 4C). The average diameter of the postcapillary venular segments analyzed is not significantly different among WKY, SHR, CGS WKY, and CGS SHR (Fig. 4D).

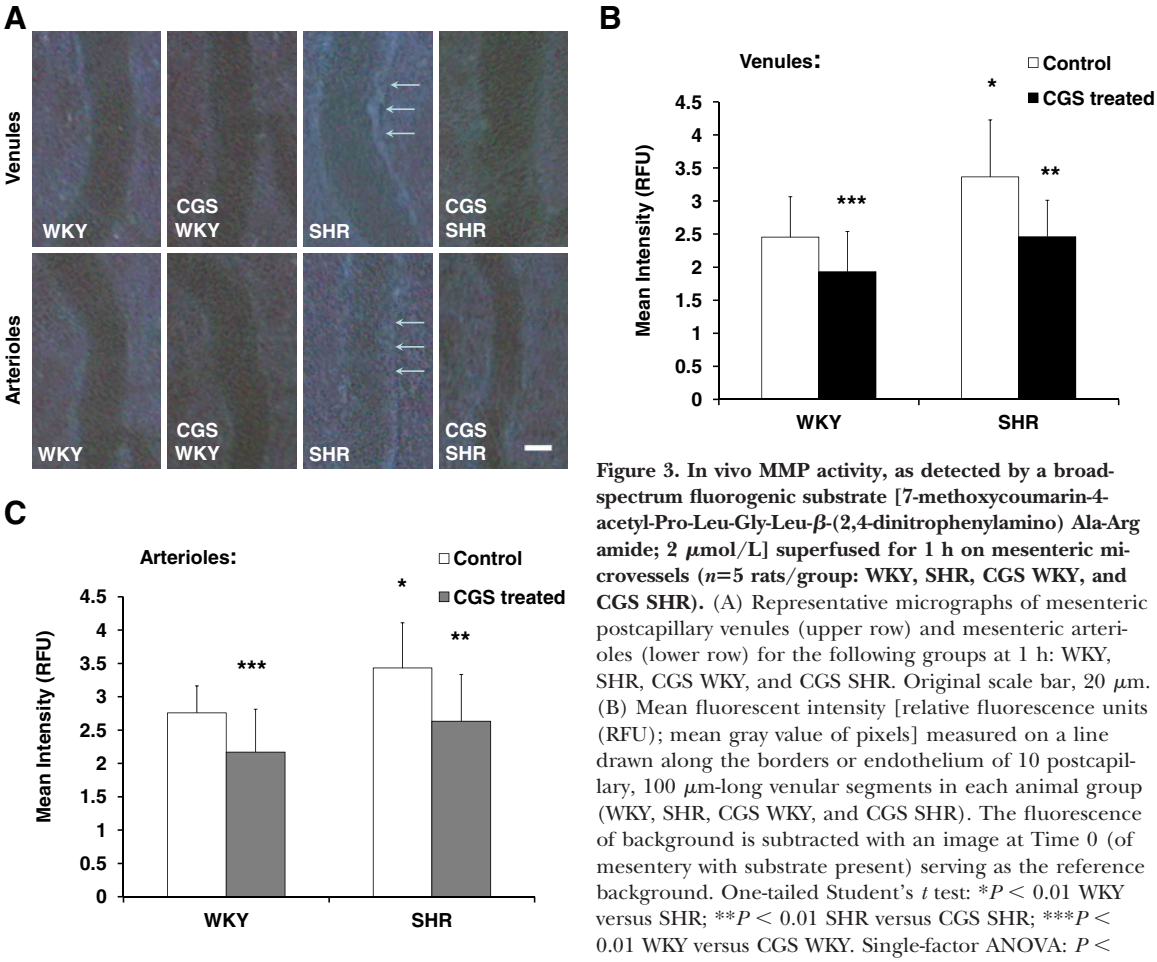


Figure 3. In vivo MMP activity, as detected by a broad-spectrum fluorogenic substrate [7-methoxycoumarin-4-acetyl-Pro-Leu-Gly-Leu-β-(2,4-dinitrophenylamino) Ala-Arg amide; 2 μmol/L] superfused for 1 h on mesenteric microvessels (n=5 rats/group: WKY, SHR, CGS WKY, and CGS SHR). (A) Representative micrographs of mesenteric postcapillary venules (upper row) and mesenteric arterioles (lower row) for the following groups at 1 h: WKY, SHR, CGS WKY, and CGS SHR. Original scale bar, 20 μm. (B) Mean fluorescent intensity [relative fluorescence units (RFU); mean gray value of pixels] measured on a line drawn along the borders or endothelium of 10 postcapillary, 100 μm-long venular segments in each animal group (WKY, SHR, CGS WKY, and CGS SHR). The fluorescence of background is subtracted with an image at Time 0 (of mesentery with substrate present) serving as the reference background. One-tailed Student's t test: *$P < 0.01$ WKY versus SHR; **$P < 0.01$ SHR versus CGS SHR; ***$P < 0.01$ WKY versus CGS WKY. Single-factor ANOVA: $P < 0.01$ among WKY, SHR, CGS WKY, and CGS SHR (not shown). (C) Mean fluorescent intensity measured with a line drawn along the borders or endothelium of 10 arteriolar, 100 μm-long segments in each animal group (WKY, SHR, CGS WKY, and CGS SHR). One-tailed Student's t test: *$P < 0.01$ WKY versus SHR; **$P < 0.01$ SHR versus CGS SHR; ***$P < 0.01$ WKY versus CGS WKY. Single-factor ANOVA: $P < 0.01$ among WKY, SHR, CGS WKY, and CGS SHR (not shown).

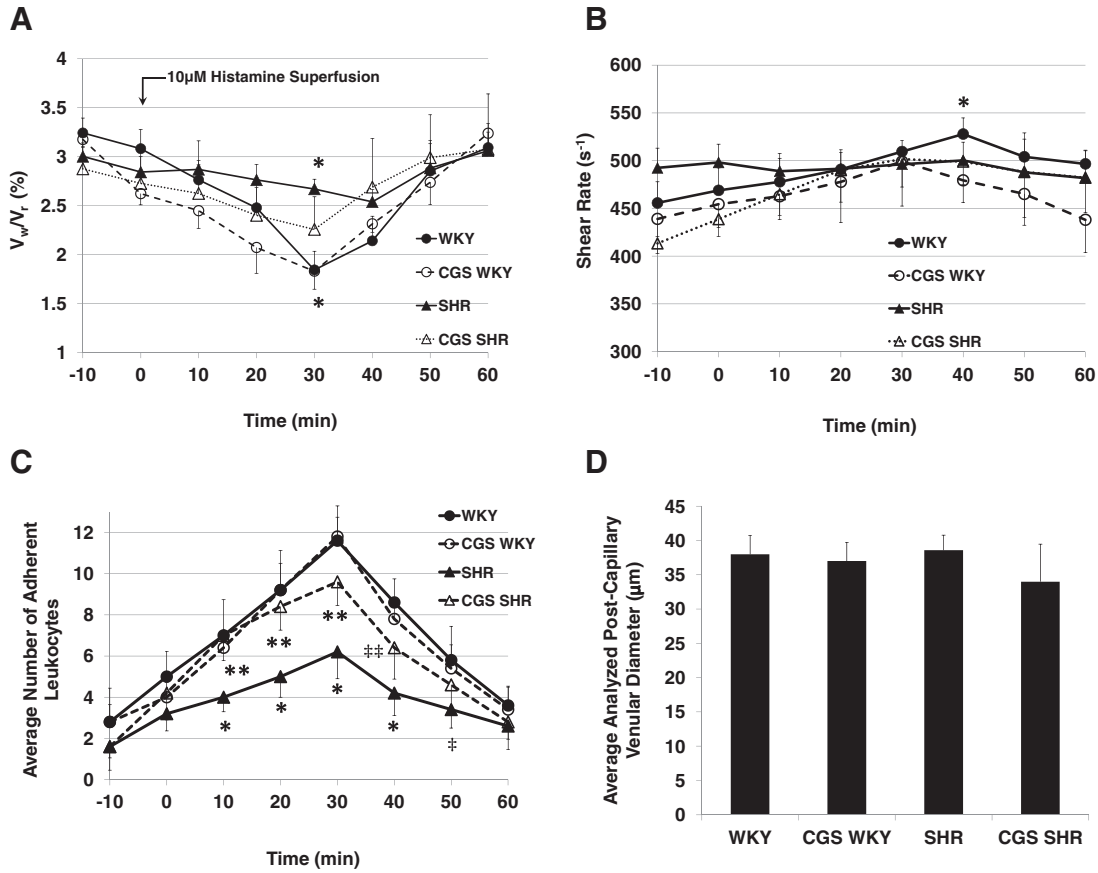


Figure 4. Leukocyte rolling velocity, venular shear rate, number of adherent cells in the postcapillary venules of WKY, SHR, CGS WKY, and CGS SHR (n=5 rats/group; n=20 leukocytes analyzed/rat and per one venular segment), and diameter of postcapillary venular segments analyzed. Histamine (10 μmol/L) was applied topically to the mesentery (via superfusion) at Time 0 min for 10 min. (A) Average leukocyte rolling velocity normalized to erythrocyte centerline velocity measured along an 80-μm venular segment in the mesenteric postcapillary venule. One-tailed Student's t test: $^*P < 0.01$ for V_w/V_R (WKY) versus V_w/V_R (SHR) at 30 min. (B) Corresponding average venular shear rates in each animal group. One-tailed Student's t test: $^*P < 0.05$ WKY versus SHR at 40 min. (C) Average number of leukocytes adherent to the endothelium along 80 μm mesenteric postcapillary venular segments at −10, 0, 10, 20, 30, 40, 50, and 60 min. One-tailed Student's t test: $^*P < 0.01$ WKY versus SHR at t = 10, 20, 30, and 40 min; $^{**}P < 0.01$ SHR versus CGS SHR at t = 10, 20, and 30 min; $^{\ddagger}P < 0.05$ WKY versus SHR at t = 50 min; $^{\ddagger\ddagger}P < 0.05$ SHR versus CGS SHR at t = 40 min. Single-factor ANOVA: $P < 0.05$ among WKY, SHR, CGS WKY, and CGS SHR (not shown). (D) Average diameter of postcapillary venular segments analyzed in WKY, SHR, CGS WKY, and CGS SHR. There are no significant differences among groups based on one-tailed Student's t test for pair-wise comparisons and single-factor ANOVA for all four groups.

MMP-9 superfusion on WKY mesenteric postcapillary venules after histamine stimulation reduces the number of adherent leukocytes

In addition to the reduction in adherent leukocyte count in the MMP-9 superfusion group (1.63 nM; **Fig. 5A** and **C**; black arrows and MMP-9 superfusion, respectively), the leukocyte rolling velocity for the MMP-9 superfusion group increased significantly compared with the PBS superfusion group at the end of the 10-min MMP-9 superfusion, reflecting the decrease in the number of adherent leukocytes (Fig. 5B; t=20 min; MMP-9 vs. PBS superfusion).

The SHR had a significantly lower extracellular P-selectin density in the postcapillary venules compared with the WKY

Chronic MMP inhibition restored the extracellular P-selectin density in the postcapillary venules of the SHR and the WKY (**Fig. 6**). On average, the SHR postcapillary venules were 31% lower in extracellular P-selectin density compared with the WKY (Fig. 6A and C). In addition, the extracellular P-selectin density on arterioles and capillaries was lower in the SHR compared with the WKY but not significantly (Fig. 6A and C, images of capillaries not shown). The negative control with IgG replacing the primary antibody had nondetectable P-selectin label density (Fig. 6B).

Labeling of the PSGL-1 by immunohistochemistry on membranes of leukocytes from fresh blood smears fixed in 10% formalin revealed a significantly reduced extracellular PSGL-1 density in the SHR

On average, the extracellular PSGL-1 domain density in the SHR was 49% lower compared with that of the WKY (**Fig. 7A**; WKY vs. SHR), and the reduced density in the SHR was significantly restored after chronic MMP inhibition (Fig. 7A; SHR vs.

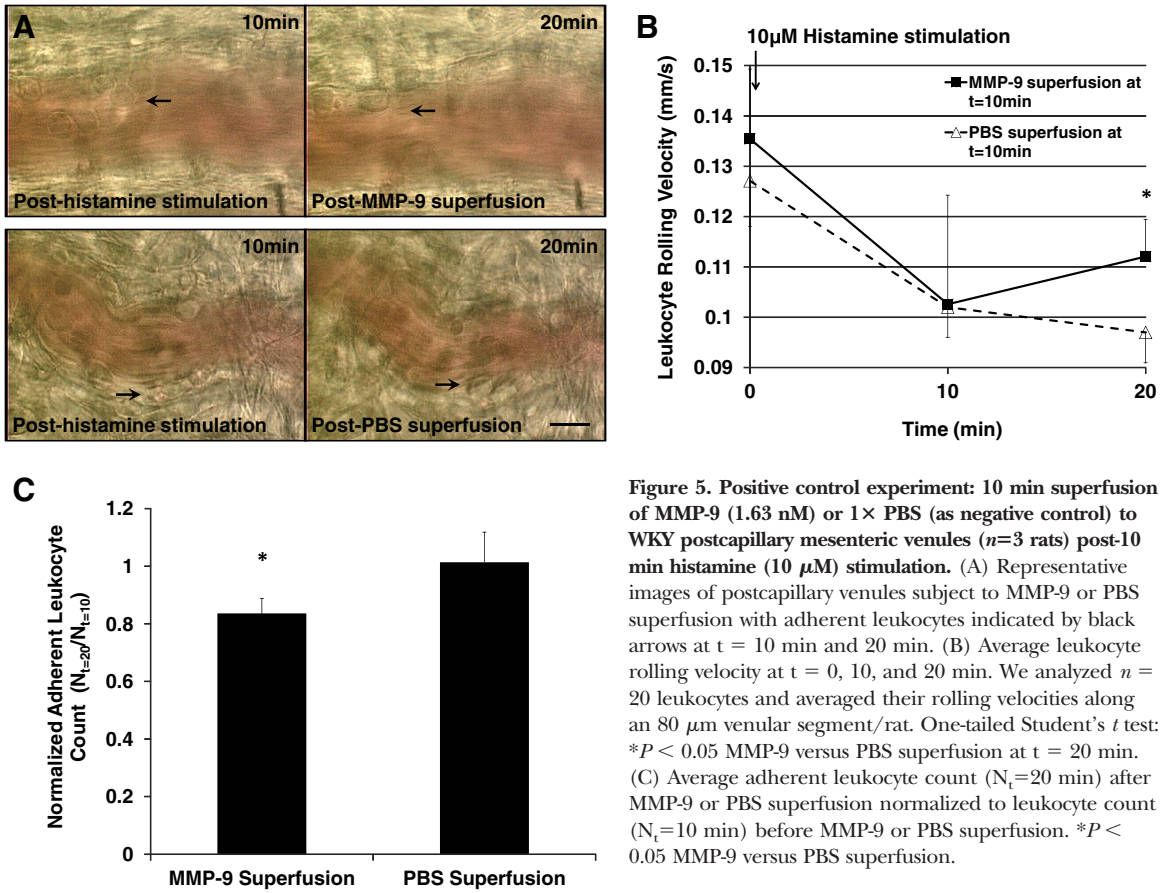


Figure 5. Positive control experiment: 10 min superfusion of MMP-9 (1.63 nM) or 1× PBS (as negative control) to WKY postcapillary mesenteric venules (n=3 rats) post-10 min histamine (10 μM) stimulation. (A) Representative images of postcapillary venules subject to MMP-9 or PBS superfusion with adherent leukocytes indicated by black arrows at t = 10 min and 20 min. (B) Average leukocyte rolling velocity at t = 0, 10, and 20 min. We analyzed n = 20 leukocytes and averaged their rolling velocities along an 80 μm venular segment/rat. One-tailed Student's t test: $^*P < 0.05$ MMP-9 versus PBS superfusion at t = 20 min. (C) Average adherent leukocyte count (N_t=20 min) after MMP-9 or PBS superfusion normalized to leukocyte count (N_t=10 min) before MMP-9 or PBS superfusion. $^*P <$ 0.05 MMP-9 versus PBS superfusion.

CGS SHR). In contrast, the intracellular domain density of PSGL-1 was not significantly different between WKY and SHR (Fig. 7B). The intracellular PSGL-1 domain labeling by immunohistochemistry also showed a small increase in density for the treatment groups compared with the control groups but not significantly (Fig. 7B; WKY vs. CGS WKY and SHR vs. CGS SHR). The negative control, with an irrelevant IgG replacing the primary antibody, showed no detectable label density (Fig. 7C). Note that the PSGL-1 label density in the extracellular and intracellular domains is heterogeneous on the cell membranes (Fig. 7A and B micrographs), a morphological feature found in receptor labeling of leukocyte membranes on blood smears.

The elevated SHR circulating leukocyte count, including PMN leukocytes and lymphocytes, is reduced after chronic MMP inhibition

Chronically CGS WKY and CGS SHR showed a reduced number of total circulating leukocytes compared with their nontreated control groups, WKY and SHR, respectively (**Fig. 8A**). The average total circulating leukocyte count of the CGS SHR group was not significantly different from the WKY controls (Fig. 8A). The average PMN leukocyte and lymphocyte count of the SHR was significantly higher than that in the WKY (Fig. 8B and C). The PMN leukocyte counts of CGS WKY and CGS SHR were significantly lower than their controls, WKY and SHR, respectively (Fig. 8B). Specifically, the difference in PMN leukocyte count between CGS SHR and SHR was larger than the difference in PMN leukocyte count between CGS WKY and WKY (Fig. 8B). The PMN leukocyte count of CGS SHR was not statistically different from that of the WKY (Fig. 8B).

The average sP-selectin level in SHR plasma was significantly higher than that of the WKY

The sP-selectin levels in plasma, as determined by ELISA, are elevated in the SHR, and it is reduced after chronic MMP inhibition (**Fig. 9**). The plasma sP-selectin levels of CGS SHR were not significantly different from that of the WKY (Fig. 9).

DISCUSSION

In the SHR, leukocytes in the postcapillary venules exhibit a blunted response upon histamine stimulation, as shown by their rolling velocities and impaired adhesion to the endothelium (Fig. 4A and 4C; WKY vs. SHR) [8, 14, 19]. The disruption of leukocyte adhesion and rolling mechanisms on the SHR endothelium is associated with elevated MMP activities, which lead to abnormal proteolytic cleavage of extracellular P-selectin and PSGL-1. Compared with the WKY, the impairment of leukocyte adhesion in the SHR correlates with an elevated SHR circulating leukocyte count (Fig. 8A–C). Chronic MMP inhibition with CGS in the drinking water of the SHR effectively normalizes the number of circulating leukocytes to

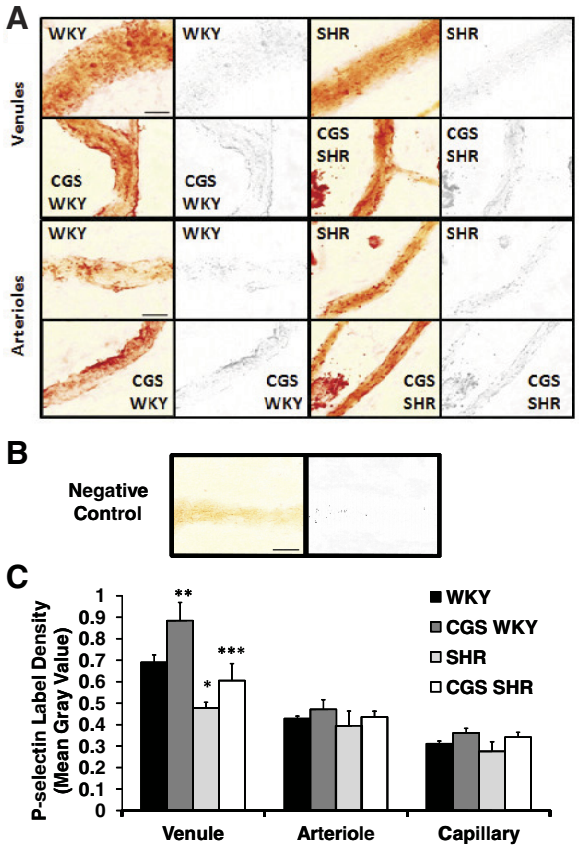


Figure 6. Whole mount mesentery microvessels labeled with extracellular P-selectin antibody using Vector NovaRED as reporter substrate. Micrographs showing an original raw image (left panels) and only P-selectin label (right panels; red channel is shown in gray scale) of A. Postcapillary venules (upper two rows) and arterioles (lower two rows) in WKY, SHR, CGS WKY, and CGS SHR (n=5 rats/group; n=1 mesentery sector/rat; n=10 vessel segments/rat). (B) Negative control (IgG). (C) Mean intensity measured from P-selectin label of mesenteric postcapillary venules, arterioles, and capillaries of WKY, SHR, CGS WKY, and CGS SHR. One-tailed Student's t test: *$P < 0.01$ WKY versus SHR; **$P < 0.05$ WKY versus CGS WKY; ***$P < 0.05$ SHR versus CGS SHR. Single-factor ANOVA: $P < 0.01$ for postcapillary venules among WKY, SHR, CGS WKY, and CGS SHR (not shown). Original scale bars in A and B, 30 μm.

levels in the WKY (Fig. 8A). Although the PMN leukocytes and the lymphocytes are elevated significantly in the SHR compared with the WKY (Fig. 8B and C), the major subtype of leukocytes, reduced significantly by CGS in the SHR, is the PMN leukocytes (Fig. 8B). The effect of CGS treatment is more prominent in the SHR compared with the WKY (Fig. 8B).

Proteolytic cleavage of the adhesion receptors, P-selectin and PSGL-1, is in line with cleavage of other vascular receptors in the SHR, such as the β_2-adrenergic receptor, the insulin receptor-α, and the FPR, resulting in arterial blood pressure elevation, insulin resistance, and impaired fluid shear stress response, respectively [10–13]. MMP cleavage of the SHR FPR is a process that leads to impairment of neutrophil pseudopod retraction under fluid shear [13]. Chemotactic stimulation with the tripeptide fMLP fails to elicit a normal pseudopod projection, reflected by actin polymerization in SHR neutrophils [13].

In addition to the FPR, the leukocyte integrin CD11b/CD18 (macrophage-1 antigen), also activated by fMLP, participates in leukocyte adherence-dependent locomotion [20]. Fluid shear stress down-regulates surface expressions of CD18 integrins and increases the chance of lysosomal proteases, such as cathepsin B, to cleave the integrin, leading to neutrophil pseudopod retraction, as well as detachment from substrates, such as the endothelium [21, 22]. In the SHR, the CD18 integrin is also defective as a result of MMP cleavage [10]. Proteolytic damage to CD18, along with its counter receptor, ICAM-1,

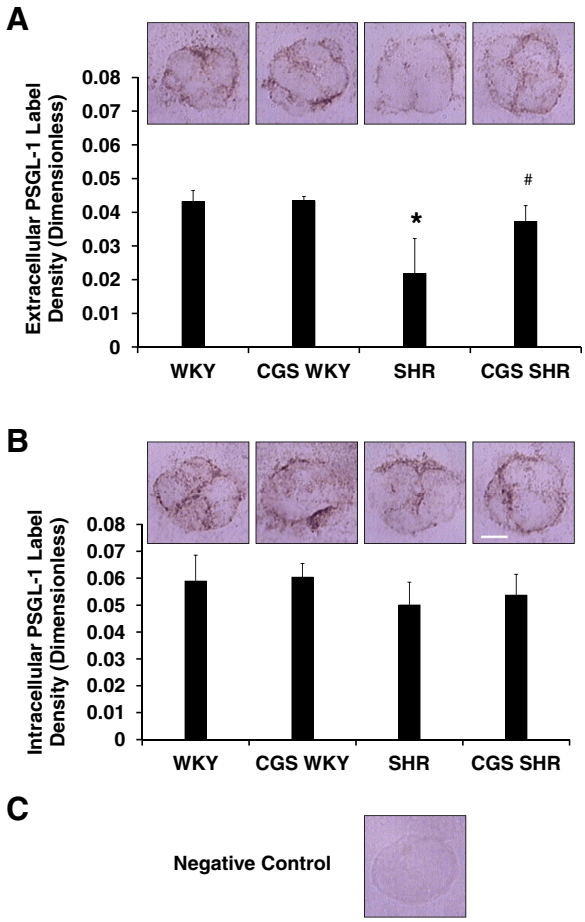


Figure 7. PSGL-1 labeling via immunohistochemistry on WKY, SHR, CGS WKY, and CGS SHR neutrophil membranes from blood smears (n=5 rats/group; n=30 neutrophils/rat). (A) Extracellular domain of PSGL-1. (B) Intracellular domain of PSGL-1. A representative neutrophil micrograph for each animal group is shown above the corresponding bar graph in A and B. Original scale bar, 5 μm. (C) Micrograph of negative control neutrophil where primary antibody was replaced by IgG. The label density for the negative control is nondetectable. The average pixel intensities were computed within the cell contours and normalized to background intensity without cells. One-tailed Student's t test: *$P < 0.05$ WKY versus SHR; #$P < 0.05$ SHR versus CGS SHR for extracellular domain PSGL-1 labeling in A. Single-factor ANOVA for extracellular domain of PSGL-1: $P < 0.01$ among WKY, SHR, CGS WKY, and CGS SHR (not shown).

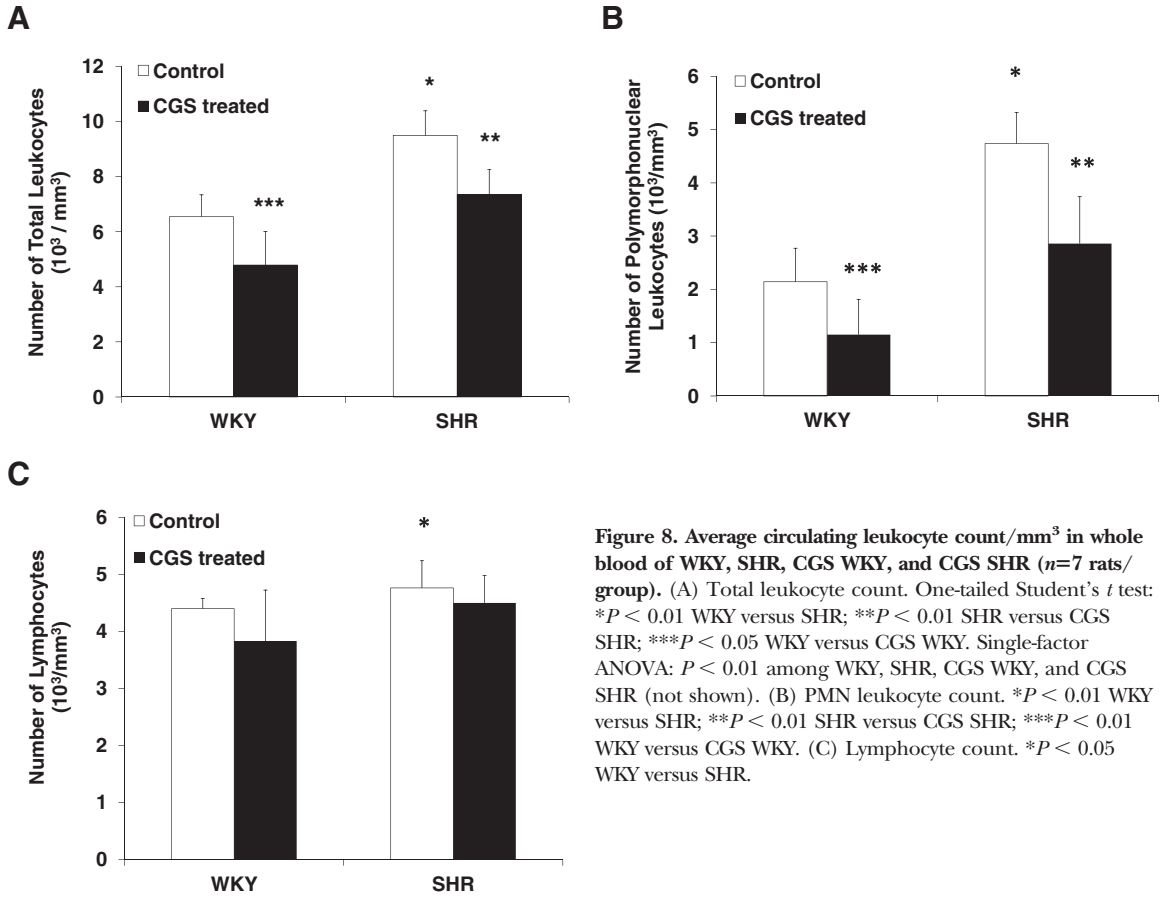


Figure 8. Average circulating leukocyte count/mm³ in whole blood of WKY, SHR, CGS WKY, and CGS SHR (n=7 rats/group). (A) Total leukocyte count. One-tailed Student's t test: $*P < 0.01$ WKY versus SHR; $**P < 0.01$ SHR versus CGS SHR; $***P < 0.05$ WKY versus CGS WKY. Single-factor ANOVA: $P < 0.01$ among WKY, SHR, CGS WKY, and CGS SHR (not shown). (B) PMN leukocyte count. $*P < 0.01$ WKY versus SHR; $**P < 0.01$ SHR versus CGS SHR; $***P < 0.01$ WKY versus CGS WKY. (C) Lymphocyte count. $*P < 0.05$ WKY versus SHR.

as well as other adhesion molecules, in the SHR may also contribute to the defective leukocyte-endothelial interaction [10, 23].

In the current study, we confirmed the presence of significantly higher MMP activities in the SHR compared with the WKY (Figs. 2 and 3), which is consistent with previous studies, showing an elevation of MMP-2, -7, and -9 in SHR plasma [10, 11]. Specifically, MMP-9 levels are significantly higher in the SHR mesenteric microvessels, as shown by immunolabeling [10]. The elevation of MMP level and activity may be transient and meal-dependent, with postmeal MMP activity significantly higher than that measured premeal in the rat (unpublished results). Regulation of MMP levels, including activation mechanisms of pro-MMPs, inhibitory mechanisms of MMPs (e.g., TIMPs), as well as transcriptional controls of MMP production, remains to be studied further [24].

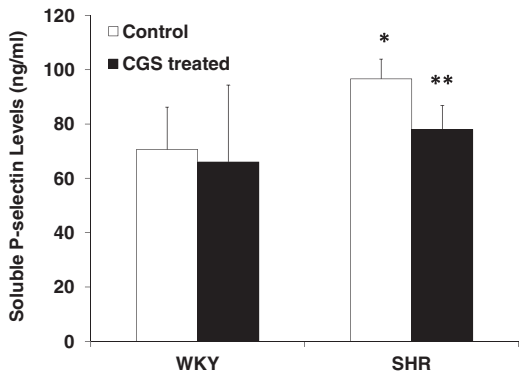


Figure 9. Average sP-selectin levels (ng/ml) in the plasma of WKY, SHR, CGS WKY, and CGS SHR (n=3 rats/group) measured by ELISA. One-tailed Student's t test: $*P < 0.05$ WKY versus SHR; $**P < 0.05$ SHR versus CGS SHR.

MMPs have the ability to cleave multiple membrane receptors on the vascular endothelium and endothelial glycocalyx [11, 25]. Although the extracellular P-selectin density was, in general, heterogeneous within animals and among animals, on the endothelium of postcapillary venules, the average extracellular P-selectin density in the SHR was significantly lower than the WKY (Fig. 6A and C). The extracellular PSGL-1 density on SHR neutrophils (Fig. 7A) was also heterogeneous. The extracellular domains of P-selectin (Protein Accession #P98106) and PSGL-1 (Protein Accession #Q8K5B0) [26, 27] contain multiple cleavage sites for MMP-9, but the exact sites, which are cleaved in vivo, remain to be determined.

The current evidence herein shows that chronic MMP inhibition interferes with the receptor cleavage phenomenon. As a synthetic hydroxamic acid derivative, the broad-spectrum MMP inhibitor CGS blocks MMP activity by binding Zn^{2+} at the active sites of a wide range of MMPs [28, 29]. The maximal tol-

erable dose of CGS in humans is 300 mg of CGS, given twice/day, which is equivalent to 10 mg/kg total/day for a 60-kg person [29]. Above this dose, patients develop a maculopapular rash, which dose-dependently increases in frequency and severity [29]. The current dose of 3 mg/kg/day CGS falls below the maximal tolerable dose and still effectively decreases plasma MMP activity in the SHR over time. After 24 weeks of treatment with CGS, the SHR presented a significantly lower systolic blood pressure, as well as a significantly reduced gelatinase and MMP activity (Figs. 1, 2, and 3A–C; SHR vs. CGS SHR). Systolic blood pressure readings via tail-cuff plethysmography were comparable with those measured from the femoral artery using a pressure transducer [10]. Furthermore, chronic MMP inhibition with CGS produced similar effects or reduction in MMP activity and systolic blood pressure for the WKY besides the SHR. The biochemical and pharmaceutical pathways, which CGS renders in control versus hypertensive animals, remain to be delineated in future studies. Moderate MMP inhibition could serve as a potential therapeutic option in normalizing systolic blood pressure, down-regulating gelatinase activity, and preventing excessive proteolytic cleavage of vascular receptors, which lead to cellular dysfunctions in hypertensives.

In this study, we used the method of immunohistochemistry for the detection of P-selectin and PSGL-1 densities rather than flow cytometry or Western blot. The major reason is that centrifugation, which is a required sample preparation step in flow cytometry and Western blot, leads to damage or shedding of receptors on neutrophils as a result of degranulation [13]. As a result, the ability to label a receptor is compromised and no longer represents the in vivo physiological state. Not only is the circulating leukocyte count of the SHR significantly higher than that of the WKY (Fig. 8A–C), but also, the SHR has endothelial apoptosis and capillary rarefaction as a result of MMP cleavage of VEGFR-2 [11]. Additional separation steps would need to be performed to equalize the number of leukocytes as well as the number of endothelial cells between WKY and SHR for comparison of PSGL-1 and P-selectin density, respectively, before using methods, such as Western blot or flow cytometry (but without centrifugation). Consequently, we used immunohistochemistry in conjunction with quantitative image analysis to detect receptor density so that whole blood and whole-mount mesentery tissues are analyzed with minimal manipulation.

Our study is driven by the hypothesis that elevated MMPs in the SHR lead to cleavage and damage of P-selectin and PSGL-1; however, there may be other mechanisms in the SHR causing impairment of leukocyte adhesion to the endothelium. First, it is possible that the ability of histamine to stimulate P-selectin is compromised as a result of defective histamine receptors, such as the H1 and H4 receptors. Endogenous inflammatory mediators, such as platelet activating factor and leukotriene B_4, have also been shown to produce attenuated leukocyte adhesion in postcapillary venules of hypertensive rats [14]. Histamine receptors (H1 and H4 receptors) are important in leukocyte recruitment in allergic inflammation, whereas the histamine H1 receptor has been shown to be critical in histamine-induced leukocyte rolling and adhesion to postcapillary venules [30, 31]. Second, platelet-mediated recruitment of leukocytes to the endothelium may depend on the vWF secreted in the SHR. It has been shown that in response to LPS stimulation, the SHR released significantly more vWF than the WKY [32]. Potential proteolytic cleavage of P-selectin on platelets could impair platelet-mediated leukocyte recruitment to the endothelium. This possibility requires further investigation in future studies.

In the SHR, cleavage of the extracellular domain of P-selectin and PSGL-1 leads to impaired leukocyte rolling after histamine stimulation and consequently, reduced adhesion and transmigration into surrounding tissues (Fig. 4A and C). Chronic MMP inhibition by CGS treatment significantly restored extracellular P-selectin density on the endothelium of postcapillary venules, extracellular PSGL-1 density on neutrophils, and leukocyte rolling in response to histamine stimulation in the SHR (Figs. 4, 6, and 7). The specific MMPs responsible for cleavage of the VEGFR-2 in the SHR include MMP-2, -7, and -9 [11]; we tested in a positive control experiment by topical application of MMP-9 (1.63 nM) on the WKY mesentery. MMP-9 appears to enter the circulation after histamine stimulation (with increased capillary permeability and leukocyte adhesion to the endothelium), causing release of adherent leukocytes from the postcapillary endothelium (Fig. 5A and C). The increased leukocyte rolling velocity after 10 min of MMP-9 superfusion (at 20 min in Fig. 5B) also correlates with the detachment of adherent leukocytes, which originally became adherent from histamine stimulation. MMP-9 may thus contribute to cleavage of extracellular domains of P-selectin on endothelial cells and PSGL-1 on leukocytes.

It is interesting to note that an impaired response of the SHR leukocytes with a reduced number of adherent neutrophils and blunted transendothelial migration has been shown to be an acute, protective mechanism against inflammation [33, 34]. The elevation of MMP activity in SHR plasma and cleavage of adhesion receptors may contribute to this protective mechanism. In contrast, studies have shown that enhanced numbers of lymphocytes and macrophages chronically infiltrate the SHR kidney and surround cerebral blood vessels of hypertensive rats [35, 36]. Infiltrations of such cell types in the SHR could initiate after renal and brain damage or may be causing complications associated with hypertension and diabetes [18, 37]. Involvement of elevated MMPs and potential receptor cleavage kinetics in lymphocytes and macrophages in the SHR remain to be examined.

An important approach to confirm receptor cleavage is by locating and quantifying the cleavage product in plasma, as soluble receptor fragments may serve as indicators for proteolytic cleavage. Present in plasma at low concentrations on the order of 100 ng/ml [38], sP-selectin requires sensitive detection methods, such as ELISA, and novel nano-scale tools [39]. Plasma concentrations of sP-selectin fragments are elevated in the SHR (Fig. 9), as well as in human hypertensives, and they have been interpreted as markers for platelet activation in cardiovascular diseases [40–44]. Our ELISA indicates that chronic MMP inhibition by CGS restores sP-selectin levels in the SHR plasma to levels found in the normotensive control WKY rat (Fig. 9). In addition to sP-selectin, soluble fragments

of its primary ligand, PSGL-1, as well as extracellular domain fragments of other receptors may provide further insights regarding the MMP cleavage phenomenon.

sPSGL-1 has been found to be higher in the supernatants of activated neutrophils, a process that reduces adhesion of leukocytes to P-selectin in vitro [45]. MMP inhibitors, such as doxycycline and EDTA, reduce sheddase (a type of metalloproteinase) activity, as well as prevent endothelial glycocalyx from shedding [25]. This leads to antiadhesion and proadhesion effects, as sheddases promote cleavage of extracellular receptor domains; shedding of glycocalyx may expose adhesion molecules that aid in adhesion [25], whereas receptor cleavage is antiadhesive (Fig. 4C; SHR). The elevated MMP level in the SHR (Figs. 2 and 3) and lower SHR extracellular domain density of P-selectin and PSGL-1 on endothelium and leukocytes, respectively (Figs. 6 and 7), indicate that receptor cleavage is likely to occur, in addition to shedding of the glycocalyx. The P-selectin$^{-/-}$ genes in animal models provide further insights about the essential role of P-selectin with respect to hypertension.

In the angiotensin II-induced form of hypertension, the P-selectin$^{-/-}$ mice, after angiotensin II infusion, have a significantly higher mean arterial blood pressure than WT control mice with saline infusion [46]. However, the mean arterial pressure of the P-selectin$^{-/-}$ mice with angiotensin II infusion is not significantly different from the WT mice infused with angiotensin II [46]. In contrast, the angiotension II-infused P-selectin$^{-/-}$ mice with WT bone marrow chimeras have a significantly reduced mean arterial blood pressure compared with the WT mice infused with angiotensin II [46]. This evidence suggests that P-selectin$^{-/-}$ mice are prone to angiotensin II-induced hypertension, and WT bone marrow P-selectin chimeras facilitate normalization of blood pressure. P-selectin$^{-/-}$ mice also have increased glomerular damage, elevated proteinuria, and higher mortality compared with WT mice [47]. In addition, elevated circulating neutrophil counts, lack of leukocyte rolling, and delayed leukocyte extravasation upon inflammatory stimulation in P-selectin$^{-/-}$ mice demonstrate immunological dysfunctions as a result of impairment of P-selectin [48]. In tissue repair mechanisms, such as wound healing, selectins and adhesion molecules play important roles by regulating inflammatory cell infiltrations [49]. P-, E-, and L-selectin$^{-/-}$ as well as ICAM-1 have been documented to delay wound healing of the skin in mice [49]. The absence of PSGL-1 (in genetically deficient mice) also inhibits early cutaneous wound healing [50]. Therefore, P-selectin and its primary ligand PSGL-1 are essential mediators in a number of physiological repair mechanisms. The SHR may be at a higher risk for impaired wound healing with an elevation of MMPs and defects in P-selectin and PSGL-1.

In summary, defects in P-selectin, PSGL-1, and integrins, in conjunction with a reduced ability to project pseudopods, may contribute to leukocyte adhesion deficiency in the SHR. During exogenous inflammatory stimuli, there were lower extracellular P-selectin and PSGL-1 receptor densities on endothelial cells and leukocytes, respectively, in the SHR compared with the WKY. The evidence not only provides a specific manifestation of immune dysfunction in the SHR but also fortifies the receptor cleavage mechanism seen with other vascular receptors as a result of elevated MMP levels in the SHR. Transcriptional regulations of MMPs, as well as P-selectin and PSGL-1, in the SHR remain to be investigated further. Pharmacological interventions in the SHR by chronically blocking MMP activity with CGS significantly reduced blood pressure, restored P-selectin density, enhanced leukocyte responses to histamine stimulation, and recovered circulating leukocyte counts.

AUTHORSHIP

A.Y.C. contributed to this manuscript with the composition of the report, as well as the design and the execution of experiments. J.N.H. contributed to this manuscript by facilitation of the execution of significant portions of the experiments. F.A.D. contributed to this manuscript with his guidance and design of experiments. G.W.S-S. served as the principal investigator of the work herein with conception, composition, guidance, and support of the project.

ACKNOWLEDGMENTS

Support for this work was provided by the U.S. National Heart Lung and Blood Institute (Grant HL-10881).

DISCLOSURES

The authors declare no conflicts of interest.

REFERENCES

1. Ley, K., Laudanna, C., Cybulsky, M. I., Nourshargh, S. (2007) Getting to the site of inflammation: the leukocyte adhesion cascade updated. *Nat. Rev. Immunol.* **7,** 678–689.
2. Cummings, R. D. (1999) Structure and function of the selectin ligand PSGL-1. *Braz. J. Med. Biol. Res.* **32,** 519–528.
3. Xia, L., Ramachandran, V., McDaniel, J. M., Nguyen, K. N., Cummings, R. D., McEver, R. P. (2003) N-terminal residues in murine P-selectin glycoprotein ligand-1 required for binding to murine P-selectin. *Blood* **101,** 552–559.
4. Hirata, T., Furie, B. C., Furie, B. (2002) P-, E-, and L-selectin mediate migration of activated CD8+ T lymphocytes into inflamed skin. *J. Immunol.* **169,** 4307–4313.
5. Suzuki, H., Suematsu, M., Schmid-Schönbein, G. W. (1999) Microvascular oxidative stress, immune reaction and apoptosis in hypertensives. *Clin. Hemorheol. Microcirc.* **21,** 161–168.
6. Schmid-Schönbein, G. W., Seiffge, D., DeLano, F. A., Shen, K., Zweifach, B. W. (1991) Leukocyte counts and activation in spontaneously hypertensive and normotensive rats. *Hypertension* **17,** 323–330.
7. Fukuda, S., Yasu, T., Kobayashi, N., Ikeda, N., Schmid-Schönbein, G. W. (2004) Contribution of fluid shear response in leukocytes to hemodynamic resistance in the spontaneously hypertensive rat. *Circ. Res.* **95,** 100–108.
8. Suematsu, M., Suzuki, H., Tamatani, T., Iigou, Y., DeLano, F. A., Miyasaka, M., Forrest, M. J., Kannagi, R., Zweifach, B. W., Ishimura, Y.. (1995) Impairment of selectin-mediated leukocyte adhesion to venular endothelium in spontaneously hypertensive rats. *J. Clin. Invest.* **96,** 2009–2016.
9. Suematsu, M., Suzuki, H., DeLano, F. A., Schmid-Schönbein, G. W. (2002) The inflammatory aspect of the microcirculation in hypertension: oxidative stress, leukocytes/endothelial interaction, apoptosis. *Microcirculation* **9,** 259–276.
10. DeLano, F. A., Schmid-Schönbein, G. W. (2008) Proteinase activity and receptor cleavage: mechanism for insulin resistance in the spontaneously hypertensive rat. *Hypertension* **52,** 415–423.
11. Tran, E. D., DeLano, F. A., Schmid-Schönbein, G. W. (2010) Enhanced matrix metalloproteinase activity in the spontaneously hypertensive rat: VEGFR-2 cleavage, endothelial apoptosis, and capillary rarefaction. *J. Vasc. Res.* **47,** 423–431.
12. Rodrigues, S. F., Tran, E. D., Fortes, Z. B., Schmid-Schönbein, G. W. (2010) Matrix metalloproteinases cleave the β2-adrenergic receptor in

spontaneously hypertensive rats. *Am. J. Physiol. Heart Circ. Physiol.* **299,** H25–H35.
13. Chen, A. Y., DeLano, F. A., Valdez, S. R., Ha, J. N., Shin, H. Y., Schmid-Schönbein, G. W. (2010) Receptor cleavage reduces the fluid shear response in neutrophils of the spontaneously hypertensive rat. *Am. J. Physiol. Cell. Physiol.* **299,** C1441–C1449.
14. Arndt, H., Smith, C. W., Granger, D. N. (1993) Leukocyte-endothelial cell adhesion in spontaneously hypertensive and normotensive rats. *Hypertension* **21,** 667–673.
15. Kasaoka, T., Nishiyama, H., Okada, M., Nakajima, M. (2008) Matrix metalloproteinase inhibitor, MMI270 (CGS27023A) inhibited hematogenic metastasis of B16 melanoma cells in both experimental and spontaneous metastasis models. *Clin. Exp. Metastasis* **25,** 827–834.
16. Knight, C. G., Willenbrock, F., Murphy, G. (1992) A novel coumarin-labelled peptide for sensitive continuous assays of the matrix metalloproteinases. *FEBS Lett.* **296,** 263–266.
17. Intaglietta, M., Breit, G. A., Tompkins, W. R. (1990) Four window differential capillary velocimetry. *Microvasc. Res.* **40,** 46–54.
18. Friese, R. S., Rao, F., Khandrika, S., Thomas, B., Ziegler, M. G., Schmid-Schönbein, G. W., O'Connor, D. T. (2009) Matrix metalloproteinases: discrete elevations in essential hypertension and hypertensive end-stage renal disease. *Clin. Exp. Hypertens.* **31,** 521–533.
19. Suzuki, H., Zweifach, B. W., Forrest, M. J., Schmid-Schönbein, G. W. (1995) Modification of leukocyte adhesion in spontaneously hypertensive rats by adrenal corticosteroids. *J. Leukoc. Biol.* **57,** 20–26.
20. Hughes, B. J., Hollers, J. C., Crockett-Torabi, E., Smith, C. W. (1992) Recruitment of CD11b/CD18 to the neutrophil surface and adherence-dependent cell locomotion. *J. Clin. Invest.* **90,** 1687–1696.
21. Shin, H. Y., Simon, S. I., Schmid-Schönbein, G. W. (2008) Fluid shear-induced activation and cleavage of CD18 during pseudopod retraction by human neutrophils. *J. Cell. Physiol.* **214,** 528–536.
22. Fukuda, S., Schmid-Schönbein, G. W. (2003) Regulation of CD18 expression on neutrophils in response to fluid shear stress. *Proc. Natl. Acad. Sci. USA* **100,** 13152–13157.
23. Tong, S., Neboori, H. J., Tran, E. D., Schmid-Schönbein, G. W. (2011) Constitutive expression and enzymatic cleavage of ICAM-1 in the spontaneously hypertensive rat. *J. Vasc. Res.* **48,** 386–396.
24. Fontana, V., Silva, P. S., Belo, V. A., Antonio, R. C., Ceron, C. S., Biagi, C., Gerlach, R. F., Tanus-Santos, J. E. (2011) Consistent alterations of circulating matrix metalloproteinases levels in untreated hypertensives and in spontaneously hypertensive rats: a relevant pharmacological target. *Basic Clin. Pharmacol. Toxicol.* **109,** 130–137.
25. Lipowsky, H. H., Sah, R., Lescanic, A. (2011) Relative roles of doxycycline and cation chelation in endothelial glycan shedding and adhesion of leukocytes. *Am. J. Physiol. Heart Circ. Physiol.* **300,** H415–H422.
26. Turk, B. E., Huang, L. L., Piro, E. T., Cantley, L. C. (2001) Determination of protease cleavage site motifs using mixture-based oriented peptide libraries. *Nat. Biotechnol.* **19,** 661–667.
27. The UniProt Consortium (2011) Ongoing and future developments at the Universal Protein Resource. *Nucleic Acids Res.* **39,** D214–D219.
28. Mizuno, S., Matsumoto, K., Li, M. Y., Nakamura, T. (2005) HGF reduces advancing lung fibrosis in mice: a potential role for MMP-dependent myofibroblast apoptosis. *FASEB J.* **19,** 580–582.
29. Levitt, N. C., Eskens, F. A., O'Byrne, K. J., Propper, D. J., Denis, L. J., Owen, S. J., Choi, L., Foekens, J. A., Wilner, S., Wood, J. M., Nakajima, M., Talbot, D. C., Steward, W. P., Harris, A. L., Verweij, J. (2001) Phase I and pharmacological study of the oral matrix metalloproteinase inhibitor, MMI270 (CGS27023A), in patients with advanced solid cancer. *Clin. Cancer Res.* **7,** 1912–1922.
30. Thurmond, R. L., Gelfand, E. W., Dunford, P. J. (2008) The role of histamine H1 and H4 receptors in allergic inflammation: the search for new antihistamines. *Nat. Rev. Drug Discov.* **7,** 41–53.
31. Asako, H., Kurose, I., Wolf, R., DeFrees, S., Zheng, Z. L., Phillips, M. L., Paulson, J. C., Granger, D. N. (1994) Role of H1 receptors and P-selectin in histamine-induced leukocyte rolling and adhesion in postcapillary venules. *J. Clin. Invest.* **93,** 1508–1515.
32. McCarron, R. M., Doron, D. A., Siren, A. L., Feuerstein, G., Heldman, E., Pollard, H. B., Spatz, M., Hallenbeck, J. M. (1994) Agonist-stimulated release of von Willebrand factor and procoagulant factor VIII in rats with and without risk factors for stroke. *Brain Res.* **647,** 265–272.
33. Suzuki, H., Zweifach, B. W., Schmid-Schönbein, G. W. (1995) Vasodilator response of mesenteric arterioles to histamine in spontaneously hypertensive rats. *Hypertension* **26,** 397–400.
34. Shichijo, K., Ito, M., Sekine, I. (1991) The mechanism of low susceptibility to stress in gastric lesions of spontaneously hypertensive rats. *Life Sci.* **49,** 2023–2029.
35. Liu, Y., Jacobowitz, D. M., Barone, F., McCarron, R., Spatz, M., Feuerstein, G., Hallenbeck, J. M., Siren, A-L. (1994) Quantitation of perivascular monocytes and macrophages around cerebral blood vessels of hypertensive and aged rats. *J. Cereb. Blood Flow Metab.* **14,** 348–352.
36. Rodríguez-Iturbea, B., Quiroza, Y., Ferrebuza, A., Parra, G., Vazirib, N. D. (2004) Evolution of renal interstitial inflammation and NF-κB activation in spontaneously hypertensive rats. *Am. J. Nephrol.* **24,** 587–594.
37. Kario, K., Ishikawa, J., Hoshide, S., Matsui, Y., Morinari, M., Eguchi, K., Ishikawa, S., Shimada, K. (2005) Diabetic brain damage in hypertension: role of renin-angiotensin system. *Hypertension* **45,** 887–893.
38. Gurbel, P. A., Kereiakes, D. J., Dalesandro, M. R., Bahr, R. D., O'Connor, C. M., Serebruany, V. L. (1999) Role of soluble and platelet-bound P-selectin in discriminating cardiac from noncardiac chest pain at presentation in the emergency department. *Am. Heart J.* **139,** 320–328.
39. Ho, J. A., Jou, A. F., Wu, L. C., Hsu, S. L. (2012) Development of an immunopredictor for the evaluation of the risk of cardiovascular diseases based on the level of soluble P-selectin. *Methods* **56,** 223–229.
40. Spencer, C. G., Gurney, D., Blann, A. D., Beevers, D. G., Lip, G. Y. (2002) von Willebrand factor, soluble P-selectin, and target organ damage in hypertension: a substudy of the Anglo-Scandinavian Cardiac Outcomes Trial (ASCOT). *Hypertension* **40,** 61–66.
41. Blann, A. D., Lip, G. Y., Fijnheer, R. (1999) Significance of soluble P-selectin, von Willebrand factor, and other adhesion molecules in hypercholesterolemia and peripheral artery disease. *Circulation* **99,** 2478–2479.
42. Lip, G. Y., Blann, A. D., Zarifis, J., Beevers, M., Lip, P. L., Beevers, D. G. (1995) Soluble adhesion molecule P-selectin and endothelial dysfunction in essential hypertension: implications for atherogenesis? A preliminary report. *J. Hypertens.* **12,** 1674–1678.
43. Semenov, A., Kogan-Ponomarev, M., Ruda, M., Komarov, A., Panchenko, E., Chazova, I., Mazurov, A. (2000) [Soluble P-selectin—a marker of platelet activation and vessel wall injury: increase of soluble P-selectin in plasma of patients with myocardial infarction, massive atherosclerosis and primary pulmonary hypertension]. *Ter. Arkh.* **72,** 15–20.
44. Varughese, G., Patel, J., Tomson, J., Blann, A., Hughes, E., Lip, G. (2007) Prognostic value of plasma soluble P-selectin and von Willebrand factor as indices of platelet activation and endothelial damage/dysfunction in high-risk patients with hypertension: a sub-study of the Anglo-Scandinavian Cardiac Outcomes Trial. *J. Intern. Med.* **261,** 384–391.
45. Davenpeck, K. L., Brummet, M. E., Hudson, S. A., Mayer, R. J., Bochner, B. S. (2000) Activation of human leukocytes reduces surface P-selectin glycoprotein ligand-1 (PSGL-1, CD162) and adhesion to P-selectin in vitro. *J. Immunol.* **165,** 2764–2772.
46. Vital, S. A., Terao, S., Nagai, M., Granger, D. N. (2010) Mechanisms underlying the cerebral microvascular responses to angiotensin II-induced hypertension. *Microcirculation* **17,** 641–649.
47. Rosenkranz, A., Mendrick, D., Cotran, R., Mayadas, T. (1999) P-selectin deficiency exacerbates experimental glomerulonephritis: a protective role for endothelial P-selectin in inflammation. *J. Clin. Invest.* **103,** 649–659.
48. Mayadas, T. N., Johnson, R. C., Rayburn, H., Hynes, R. O., Wagner, D. D. (1993) Leukocyte rolling and extravasation are severely compromised in P selectin-deficient mice. *Cell* **74,** 541–554.
49. Yukami, T., Hasegawa, M., Matsushita, Y., Fujita, T., Matsushita, T., Horikawa, M., Komura, K., Yanaba, K., Hamaguchi, Y., Nagaoka, T., Ogawa, F., Fujimoto, M., Steeber, D. A., Tedder, T. F., Takehara, K., Sato, S. (2007) Endothelial selectins regulate skin wound healing in cooperation with L-selectin and ICAM-1. *J. Leukoc. Biol.* **82,** 519–531.
50. Tomita, H., Iwata, Y., Ogawa, F., Komura, K., Shimizu, K., Yoshizaki, A., Hara, T., Muroi, E., Yanaba, K., Bae, S., Takenaka, M., Hasegawa, M., Fujimoto, M., Sato, S. (2009) P-selectin glycoprotein ligand-1 contributes to wound healing predominantly as a P-selectin ligand and partly as an E-selectin ligand. *J. Investig. Dermatol.* **129,** 2059–2067.

KEY WORDS:
glycoprotein ligand 1 · matrix metalloproteinase · mesentery · extracellular receptor density · leukocyte rolling · MMP inhibitor